28 May 2010, 2:00 pm - 3:30 pm

Fault Hazard Characterization for a Transportation Tunnel Project in Coronado, California

James R. Gingery
Kleinfelder West, Inc., San Diego, CA/University of California at San Diego, La Jolla, CA

Scott H. Rugg
Kleinfelder West, Inc., San Diego, CA

Thomas K. Rockwell
Earth Consultants International/ San Diego State University, San Diego, CA

Bruce R. Hilton
Kleinfelder West, Inc., San Diego, CA


Fifth International Conference on
Recent Advances in Geotechnical Earthquake Engineering and Soil Dynamics
and Symposium in Honor of Professor I.M. Idriss
May 24-29, 2010 • San Diego, California

FAULT HAZARD CHARACTERIZATION FOR A TRANSPORTATION TUNNEL PROJECT IN CORONADO, CALIFORNIA

James R. Gingery
Kleinfelder West, Inc.
San Diego, California-USA 92122
and University of California San Diego

Scott H. Rugg
Kleinfelder West, Inc.
San Diego, Califonria-USA 92122

Bruce R. Hilton
Kleinfelder West, Inc.
Sacramento, Caliofornia,-USA 95827

Thomas K. Rockwell
Earth Consultants International
and San Diego State University San Diego, California-USA 92182

ABSTRACT

This paper presents the results of a fault hazard study performed as part of a proposed traffic tunnel project in Coronado, California. The 2.3 km alignment crosses the Coronado fault, which is considered active by the California Geological Survey. Although the location of the Coronado fault offshore of Coronado had been well established through previous studies, the fault had never been definitively located on land. A study was undertaken that utilized four principal investigation methods: a seismic reflection survey, large diameter borings, closely-spaced cone penetrometer tests (CPT) and a fault trench. This study was the first to positively locate the Coronado fault on land and to show that approximately 29 cm of vertical displacement has occurred in the Holocene. The field investigation provided evidence that strike slip displacement has also occurred. For design purposes, the strike slip offset was estimated using an empirical model and several kinematic models that integrated aspects of the local tectonic regime. Fault offset design criteria were established for the project that accounted for uncertainty in the fault zone location and the potential for secondary faulting outside the primary fault zone.

INTRODUCTION

The City of Coronado has initiated the State Route 75/282 Transportation Corridor Project to improve traffic flow between the San Diego-Coronado Bay Bridge and the Naval Air Station North Island (NASNI), a distance of approximately 2.3 km (Figure 1). The project is in the Project Report / Environmental Document (PR/ED) phase. As such, several alignments and construction method options are under consideration. The two major project configuration options are: a cut-and-cover tunnel alignment; and a twin-bored tunnel alignment. Schematic cross-sections for these options are shown on Figure 2 and Figure 3.

This paper presents the results of a fault rupture hazard evaluation for the Coronado fault, which crosses the proposed tunnel alignment. This study was undertaken by Kleinfelder and Earth Consultants International for the prime designer, Parsons Brinckerhoff and the owner, the City of Coronado. The results of this study were used in the preliminary seismic design of tunnel alternatives.

BACKGROUND AND PREVIOUS STUDIES

A fault had long been suspected across the east side of Coronado along a prominent topographic lineament (Kennedy et al., 1977) that extends from the southwestern ocean shore near the Hotel Del Coronado northward to the bay shore near the old ferry landing (Figure 4). This lineament has been interpreted as a normal fault scarp with the hanging wall to the east (Kennedy and Welday 1980). The first hard evidence for the Coronado fault came from offshore seismic reflection data collected during a study by Kennedy and Welday (1980) in the Pacific Ocean south of Coronado. These data indicated two parallel faults offshore of the Hotel Del Coronado, closely aligned with the onshore topographic lineament. This prompted a fault study by Artim and Streiff (1981) who excavated a 60-m long trench across the suspected fault scarp at a site on 6th Street. Their logs show uniform and continuous stratigraphy, and no faults were identified within the trench. Kennedy and Clarke (1999) performed additional detailed offshore seismic reflection work, along with drilling and soil sampling, as part of a seismic hazard study for the San Diego-Coronado Bridge. Seismic profiles show traces of the

three bay faults extending upward to very near the bay floor. Age dating of sampled shell material indicated that all three faults offset Holocene sediments. The Coronado fault was considered as one of the most youthful of the three faults in the Kennedy study. The data from this previous work and others led to the classification of the Coronado fault as an active earthquake fault zone according to California Geologic Survey criteria (Treiman, 2003 and 2004). Because active faulting was not observed in a trench performed across the suspected fault scarp, Treiman (2003, 2004) mapped the active trace east of the apparent scarp with the supposition that erosion had regressed the scarp west of the fault trace.

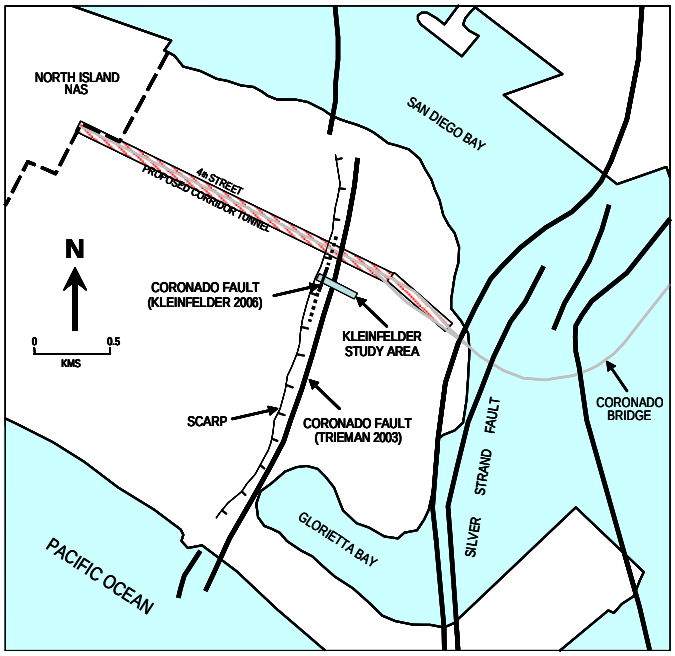

Fig. 1 – Project alignment and faulting.

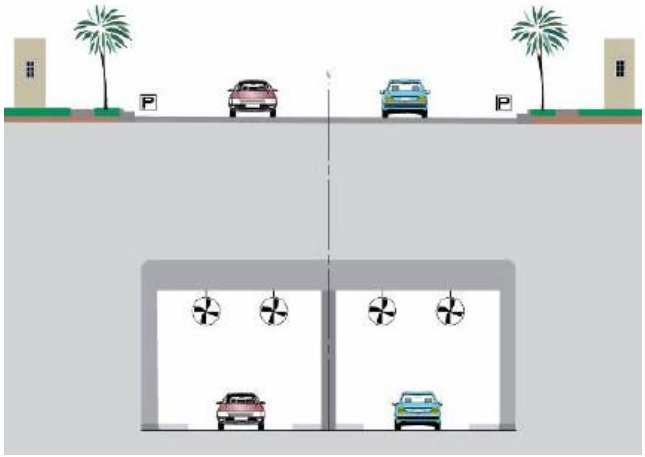

Fig. 2 – Cut and cover option.

Two parallel north-south trending sister faults that cross the Coronado peninsula, the Spanish Bight fault and the Silver Strand fault, were also classified as active by Treiman (2003, 2004). Two faults in downtown San Diego across the bay from Coronado, the San Diego fault and the Downtown Graben fault, were also classified as active faults at the same time. All of these faults are part of the Rose Canyon Fault Zone (RCFZ) near its southern terminus.

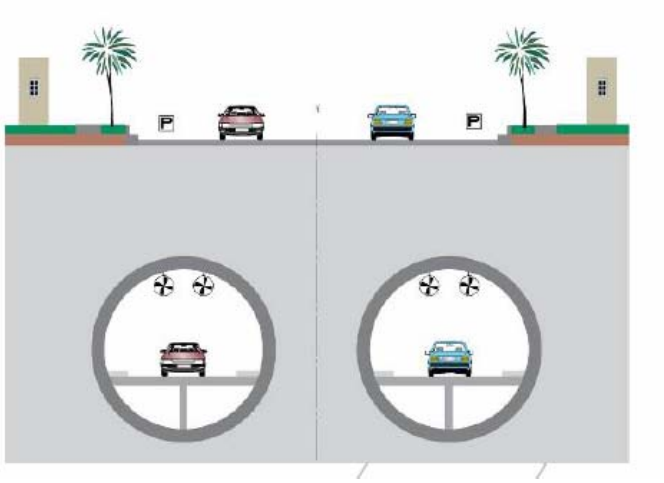

Fig. 3 – Twin bored tunnel option.

GEOLOGIC SETTING

The western coastal zone of San Diego County is dominated by a westward thickening wedge of sedimentary units that were deposited on a basement complex of igneous and metamorphic rocks. These sedimentary units can be divided into three packages based on their sequence and age of deposition. The oldest sequence consists of claystone, siltstone, sandstone, and conglomerate deposited during late Cretaceous time as an apparent submarine fan (Abbott 1999). These units crop out on Mt. Soledad in La Jolla, Point Loma and Carlsbad. The second sequence of sediments was deposited during the Tertiary (Eocene and Pliocene) within an embayment that stretched from at least northern San Diego County and southward into Mexico (Kennedy 1975). The sediments consist of a variety of claystone, siltstone, sandstone and conglomerate.

The most recent sedimentary deposits consist of early to late Pleistocene near shore marine, estuarine, and delta deposits. Most of these sediments were deposited on wave cut surfaces developed in response to sea level fluctuations during the Quaternary.

The Coronado peninsula is underlain by late Pleistocene marine terrace and near shore terrestrial deposits known as the Bay Point Formation. These units were most likely laid down during interglacial stages 5e and 7 (120ka to 220ka years BP) (Kern and Rockwell, 1992) with Coronado being an elevated sand berm feature that has prevailed to the present. Drilling performed in San Diego Bay during the seismic retrofit of the Coronado Bridge (Caltrans 1998) encountered over 50 m of late Pleistocene sediments without penetrating their base. The

considerable thickness of the unit is likely due to deposition within a down-dropped faulted-bounded basin, with the Point Loma fault on the west and the La Nacion fault on the east. The Bay Point Formation most likely overlies the Plio-Pleistocene San Diego Formation.

TECTONIC SETTING

Southern California is dominated by a wide zone of deformation associated with strain release across seven principal faults comprising the San Andreas Fault System (SAFS). The SAFS is a nearly 240 km-wide boundary separating the Pacific Plate on the west and the North American Plate on the east, spanning from the main San Andreas fault in the Imperial Valley to well offshore to the San Clemente fault. Geodetic data indicate that up to 49 mm/yr of right-lateral displacement occurs across the SAFS. Up to 84% of this displacement (41mm) occurs along the three principal faults to the east (Elsinore, San Jacinto, and San Andreas faults). The remaining 8 mm/yr of displacement is accommodated across the four faults (Rose Canyon, Coronado Banks, San Diego Through and San Clement faults) on the west (Bennett, et al., 1996).

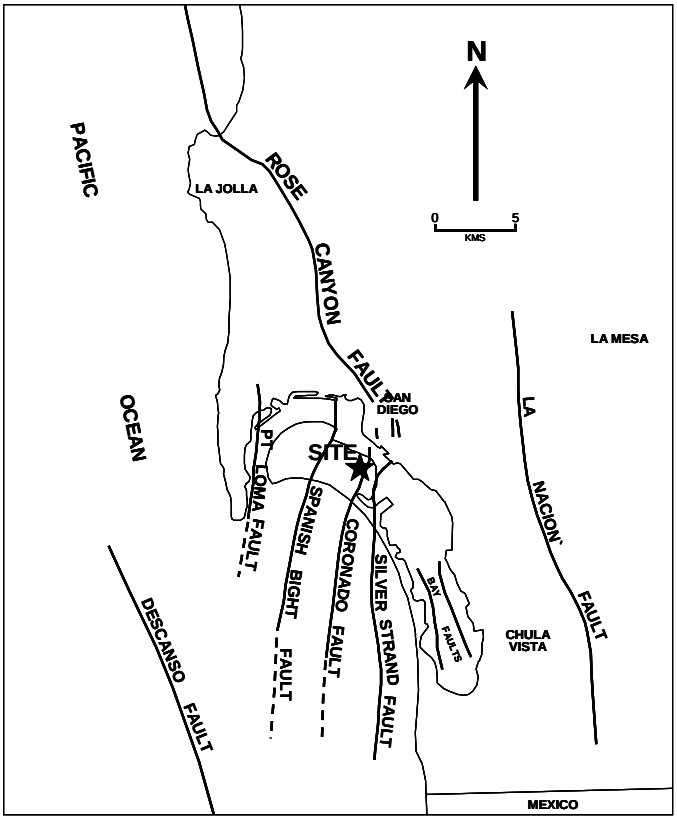

Fig. 5 – Regional fault map.

Trends of the three San Diego Bay faults indicate connectivity with active faults in downtown San Diego (Coronado and Silver Strand) or the Old Town fault to the north (Spanish Bight). One of the most conspicuous features of the bay faults is that they trend from nearly directly north to northeast at an angle (up to 40 degrees) that is noticeably different from the primary, generally northwest trend of the RCFZ (Figure 5). This suggests that these three faults may act as step-over faults between the Rose Canyon fault and offshore faults to the southwest, such as the San Miguel-Vallecitos fault or the Descanso fault.

FIELD INVESTIGATION

A phased approach to field investigation was adopted for this study. Four principal investigation methods were employed in the following order: a seismic reflection survey, large diameter borings, closely-spaced CPT's and a fault trench.

A shear wave seismic reflection study was performed along the fault zone on 4th Street during a preliminary phase. The reflection data revealed several offset reflectors which were interpreted as faults or fault-like features. However, the data was not conclusive enough to adequately constrain the fault location and displacement potential for design.

Clean fine sands with little to no cementation, along with shallow groundwater, were expected at the site. With these conditions it was questionable whether adequate stability could be achieved in an exploratory fault trench. It was also questionable whether adequate stratification would be present for fault identification. Therefore, three large diameter borings were performed to test the feasibility of trenching and fault mapping at the site. Three 60 cm borings were penetrated to depths of up to 6.1 m below ground surface. The top of boring elevations ranged from 3.4 to 8.5 m above mean sea level (MSL) with a minimum bottom elevation of 1.2 m MSL. Groundwater was encountered in one of the borings at an elevation of 1.8 m MSL. The materials consist mostly of massive unconsolidated sands with isolated layers of finely laminated micaceous sand and abundant late Pleistocene illuviated clay concentrated in B horizon laminations (B-lams). The micaceous sand layers and B-lams appeared to provide adequate horizontal markers to make dip-slip faulting observable in a trench. The stand-up time of the boring sidewalls was limited and caving occurred at several locations, indicating that shoring would be required in an exploratory trench.

In the next phase, 36 CPT soundings were performed along a 220 m alignment within 5th Street, between A Avenue on the west and Pamona Street on the east. The CPTs extended to depths ranging between 18 and 37 m below ground surface (bgs). The surface profile elevations ranged from approximately 9.1 m MSL near A Avenue to 5.5 m MSL near Pamona. Initially 26 CPT soundings spaced approximately 9.1 m apart were completed. The penetration resistance and soil identification data were then plotted and reviewed as the field investigation progressed to identify areas of potential faulting. In areas where the initial CPT data suggested faulting was present, secondary and tertiary CPT soundings were performed to provide increased resolution. CPT spacing as close as 2.3 m was performed. The data showed a clearly

defined zone of faulting extending upward to where it approached the ground surface. The faulted zone coincided with the location of the topographic lineament. Several distinct geologic horizons were offset within this zone (discussed in more detail later). Outside this zone, the horizons were found to be uniform and nearly horizontal. Figure 7 shows a profile of CPT tip resistance.

Fig. 6. Sequential shoring operations in fast-raveling sands.

Based on the CPT data, an exploratory trench excavation was made. The trench was 24 m in length and bracketed the CPT-interpreted fault zone by approximately 6 m on either side. The trench was excavated to a depth of 4 to 4.3 m. Due to the presence of clean, weakly cemented sand that was prone to fast raveling, hydraulic aluminum shoring with integrated finform panels (1.2 by 3.7 m) was required to protect the trench from collapse. The trench had to be excavated in short section sequences (1.2 m) with the shoring placed progressively as the trenching proceeded (Figure 6). The southern trench wall was first "cleaned" by scraping the lowermost exposed 60 cm of the sidewall, as well as the open spaces between adjacent shoring panels. A gauged string line was installed across the bottom of the trench in several level steps to provide both vertical and horizontal control during logging. After the trench walls were cleaned and the points of reference were established, the exposed sidewall surfaces were logged. During the logging, several prominent fault features located within the western side of the trench were identified for more detailed study. Shoring panels were removed one at a time so that detailed logging could be performed in the fault feature area. After the panels were removed, a gauged string grid system was installed in the sidewalls of the exposure and photographs were taken. After each area was logged, the shore panel was replaced and then the next panel was removed for logging. Shoring panels were only removed for detailed logging where fault features were observed extending upward from the base of the trench to behind the panels.

TRENCH STRATIGRAPHY

Several geologic and soil units were identified within the trench excavation. These units consisted of two depositional units, several superposed pedogenic soil horizons, and anthropogenic fill soils. These units are described in the following paragraphs, starting with the oldest depositional unit through the most recent soil unit.

Near Shore Marine Sand (Qbp)

The oldest unit encountered was a massively bedded, well sorted sand of probable marine origin. This interpretation is based on the observation that near the base of the trench, the sand contains horizontally bedded fine silty sand beds that are considered to have been worked in a near shore marine environment. Additionally, the sand contained shell fragments, and entire bivalves were recovered from the sand within the large diameter borings. The more massively bedded, well-sorted sand could also be, in part, aeolian in origin (beach dune environment), especially near the surface. This unit comprises most of the natural deposits exposed in the trench, and is the parent material for the soil that developed through the sand during the subsequent period of surface stability. The age of this unit is believed to be about 120 ka, based on the faunal assemblage and correlation to similar deposits elsewhere on Coronado (Kennedy 2006).

Colluvium

A relatively thin surficial colluvial deposit, consisting mostly of fine silty sand, was encountered above the marine sand along the eastern half of the trench, thickening across the fault scarp. This unit was likely developed by deposition of soil material transported by sheet flow runoff toward the east, over the face of the fault-generated scarp. The colluvium thickens and merges with the A horizon towards the east, with a maximum thickness in the trench of up to 1.2 m. This unit has also been altered by pedogenic processes (minor organic matter accumulation) and has not been differentiated from the A horizon within the central and eastern portions of the trench. The differences between the colluvium and the A-horizon are very subtle. The upper 0.5 to 0.8 m of the trench is underlain by artificial fill placed during grading of the roadway.

Asphalt Concrete and Fill (AC, AF1, AF2)

Asphalt concrete and fill associated with the asphalt pavement sections were encountered at the surface.

Pedogenic Soil Horizons

The entire section within the trench was overprinted to varying degrees by at least two phases of late Pleistocene and Holocene pedogenesis (soil development). The change in phase is likely due to the change in climate and vegetation from the Pleistocene to the Holocene (Rockwell et al., 1985; Rockwell 2000). Pedogenic processes altered the upper section of the sand through oxidation, the accumulation of illuvial clay concentrated in a laminar B horizon (B-lams), the development of the uppermost A horizon and an eluviated E horizon. For this soil section, most of the B horizon formed in the late Pleistocene, with only minor Holocene accumulation of pedogenic clay, part of which is superposed on the E horizon. The A and E horizons are also relict of Pleistocene soil development, but the E horizon is now accumulating clay in the form of thin (1-5 mm-thick) clay lams and the A horizon is constantly rejuvenated through active bioturbative processes. Therefore, when a pedogenic horizon is ascribed an age such as Holocene or Pleistocene, it is meant that this is the time frame during which the horizon developed. Soil horizons are considered active and are continually undergoing modification and development within geologic time frames.

B-Lam Horizon. The marine sand has been affected by two separate phases of pedogenic soil development. The first phase is evident by the presence of very well developed clay rich B-lams developed during the late Pleistocene under wetter conditions and probably coniferous vegetation (Huesser, 1978). The B-lams are generally horizontal and range up to 7.5 cms in thickness, and up to 3 m in length. The second phase of pedogenesis occurred during the Holocene, after southern California's climate dried out, and resulted in the formation of thin B-lams superposed on the Pleistocene E horizon. Offsets of the B-lams provided strong indicators of faulting within the trench.

E Horizon. An E horizon directly overlies the B-lam horizon and is interpreted to be largely a relic feature associated with the Pleistocene soil. E horizons typically form in intensely leached conifer forest environments (Alfisols), resulting in a character similar to the original parent material, which in this case is light gray sand. It is distinguished from the A horizon and underlying B-lam horizon by a distinctive light gray hue and the general lack of organic accumulation relative to the A horizon. Superposed on the Pleistocene E horizon are a number of thin (1-5 mm thick) incipient clay lams that are almost certainly of Holocene age.

A Horizon. The natural soil profile exposed in the trench is capped by an active and youthful Holocene-age A horizon of light, grayish-brown, silty sand. The color is clearly related to some accumulation of organic matter, and the texture is massive and uniform with pinhole to 1 mm-size void spaces which probably represent old root casts. The maximum thickness of the A horizon is about 0.6 m.

In general, recognition of pedogenic horizons and features within the exposed section allowed for a better interpretation of faulting. Some pedogenic features postdate motion on some faults, whereas others are clearly displaced, as discussed below. Thus, the soil profile provided a critical aspect that allowed quantification of the recency and timing of some fault strands, which was ultimately important in the development of possible rupture parameters.

INTERPRETATIONS OF FAULTING

The CPT data revealed several prominent and continuous depositional units east and west of the scarp, which when traced into the expected area of faulting, could be used to measure vertical displacement across the fault (Figure 7). Several fault features were identified, with the most significant located toward the west, upper side of the topographic lineament. These faults consist of two or more strands that appear to be part of a branching upward flower structure. The structure widens from a width of 2.1 m at a depth of 23 m bgs (-15.2 m MSL) to a width of approximately 13.7 m near the ground surface. The faulting in the CPT data could be followed to within 6 m of the ground surface. The sense of bedding displacement is down to the east with a maximum vertical separation of up to 6.1 m in the lowest part of the CPT section. The amount of vertical offset appears to lessen upward, which would indicate some faulting to be contemporaneous with deposition. The dip of the fault is steeply inclined toward the east, suggesting a normal component of displacement. Three other faults were identified to the west of the flower structure below the crest of the fault scarp. These faults were found to offset bedded units upward to a depth of about 14.6 m bgs (-6 m MSL), indicating that they are buried and probably inactive.

The fault trench was positioned across the area bracketing the suspected flower structure identified in the CPT data. Many fault features were exposed in the trench extending a lateral distance of up to 13.7 m in the central portion of the trench (Figure 8). The most prominent area of faulting was along a 4 m section within the western half of the trench.

Faults were visually identified along the bottom of the trench below the panel shoring by locating truncations across the B-lam layers. In particular, faults were traced upwards by identifying adjacent overlying truncated B-lams. The openings between the shoring panels were also checked for faults in a similar fashion. Suspected fault areas could also be ascertained across shore-paneled areas by abrupt elevation changes across B-lam packages and other layered geologic and soil units. The sand along the zone of truncation was found to be very loose and more prone to caving, providing more evidence for the presence of a fault.

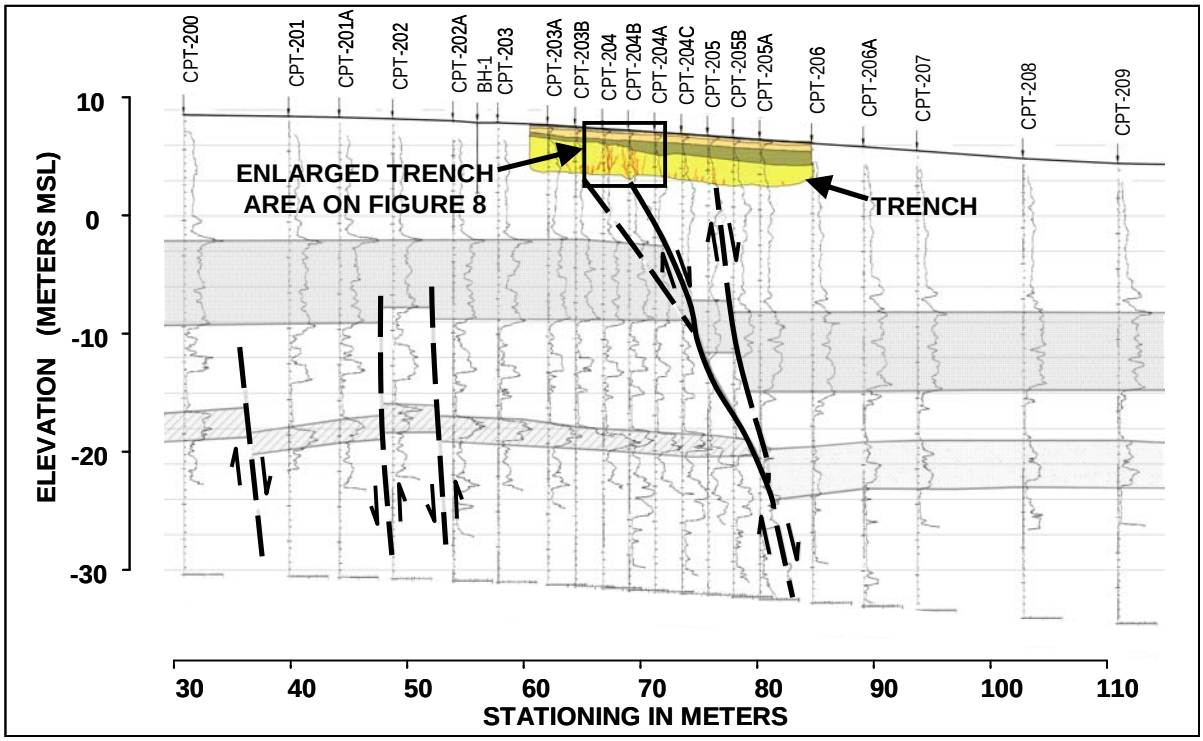

Fig. 7 – Profile showing CPT tip resistance, interpreted faulting and trench location.

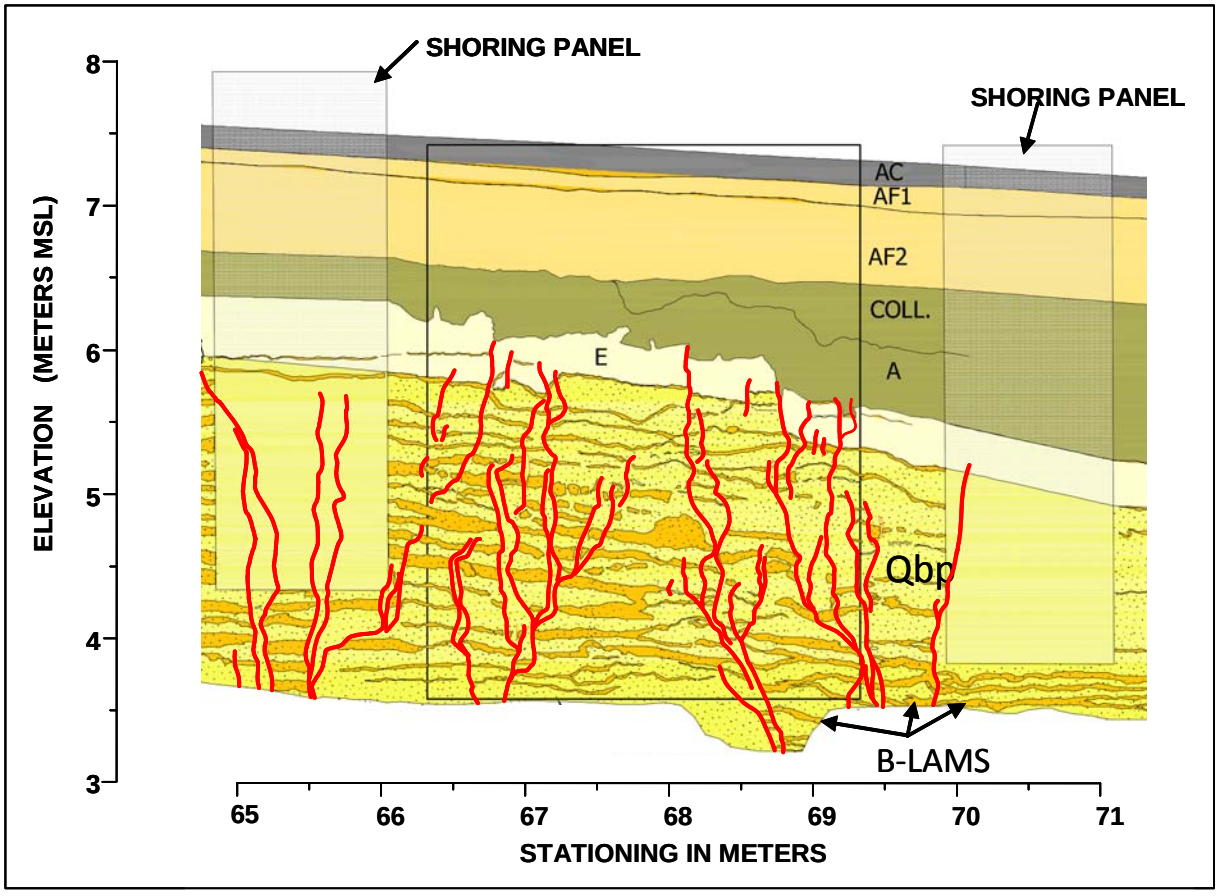

Fig. 8 – Trench log.

The general age of faulting was assessed during the initial logging by observation of the sharpness of the truncation breaks across the B-lams. The sharpest truncation breaks were observed on faults on the west side of the trench. The apparent fault structures to the east were found to be much more diffuse, with indications of "healing" across some B-lams (post faulting B-lam reformation). Reformation across deep B-lam layers indicates that these fault structures are late Pleistocene in age and have not undergone Holocene displacement. The A and E horizons above these eastern faults were observed to be uniform in thickness and did not show notable elevation changes across the openings between shore panels, suggesting that these fault strands have experience little or no motion in the Holocene.

Seven shore panels were sequentially removed, starting from the west end of the trench, to allow for detailed logging of the exposed trench sidewall in the more critical fault zone area. Fault lines were traced upwards by following B-lam truncations into the active A and E horizons, which also showed clear fault displacement across a 1.2 m zone. Two meters of topographic relief along the base of the A and E horizons was also present directly west of this zone. Cumulative vertical displacement (vertical throw) across these fault structures is a total of 29 cm at the base of the active A horizon, with less vertical movement noted to the east. The A horizon is an active "healing" zone which is continually undergoing modification due to a number of processes such as bioturbation. Therefore it can be reasonably assumed that evidence of faulting older than several hundreds of years would be obscured within the A horizon. Any sharp offsets within the A horizon would therefore suggest fault displacement within the last several hundreds of years, such as observed in the trench across the 1.2 m fault zone. There was an absence of evidence that the measured vertical offset occurred in more than one event, so for design it was conservatively assumed that the 29 cm of measured vertical throw could occur in a single event.

West of this area the faults were traced upwards, but did not appear to penetrate and displace the A and E soil horizons. These features probably represent an earlier period of faulting (possibly multiple events) in early Holocene or late Pleistocene time.

Reliable strike and dip readings could not be obtained for individual fault strands across the trench. Readings that were taken varied widely, which is characteristic of branching fault strands as they approach the surface, especially in loose sand between the clay lamellae. However, the combined CPT and trench data indicated a dip on the main fault trace of approximately 70 degrees toward the east (normal component of faulting).

Lateral (strike) separation could not be plainly measured. However, mismatch of individual B-lams and B-lam packages was observed across many faults, indicating some component of lateral slip. From a larger scale, the overall mismatch can be considered relatively small, although it is not clear how much variation is expected over tens of meters and therefore these variations cannot be used to even make general statements regarding the amount or direction of lateral displacement. Therefore, estimates of potential strike slip magnitude were made using theoretical models as described below.

STRIKE SLIP ESTIMATIONS

Horizontal displacement along the fault could not be ascertained directly through trench observations alone, because no piercing points were observed in the trench and because post-depositional pedogenic clay laminations are formed in an essentially horizontal configuration. However, the laminations did display some pinching and/or unique morphology across fault splays on the same trench wall, suggesting that the normal component of slip is accompanied by some lateral slip (see Figures 7 and 8). Horizontal displacement has not been directly observed in any of the previous studies along the Coronado fault largely because these studies utilized drilling, CPT, and/or geophysical methods incapable of detecting horizontal displacements. This is also true of the adjacent Silver Strand and Spanish Bight faults. Microseismicity studies of earthquakes swarms during 1985 to 1987 in San Diego Bay indicated left lateral movement on a system of unnamed northeast striking faults below the southern area of the bay (Magistrale, 1993). Although the Coronado fault trends more northerly rather than northeasterly and exhibits a normal rather than reverse component of slip, the Magistrale (1993) data provide another indicator that strike slip motion likely occurs on the Coronado fault.

Four deterministic methods of analysis were considered to assess the possible sense and magnitude of lateral displacement values for the Coronado fault. These methods included: 1) an independent rupture model that uses the Wells and Coppersmith (1994) empirical relationships between fault length and displacement; 2) an extensional pull-apart kinematic model that relates observed normal displacement to strike slip displacement on the Coronado fault; 3) a wrench faulting kinematic model; and 4) a "horsetail" model that distributes right lateral strike slip on the Rose Canyon fault among the Spanish Bight, Coronado, Silver Strand and various unnamed faults in the San Diego Bay. These models are discussed in the following sections.

Wells and Coppersmith Independent Rupture Model

Wells and Coppersmith (1994) complied data from worldwide historical earthquakes and developed empirical correlations between moment magnitude, surface rupture length, rupture area, and maximum and average displacement. The Wells & Coppersmith relationship for strike slip faults that relates

average and maximum displacement per event to surface rupture length was used in this study. Note that the average and maximum displacements are based on the variation of displacement that typically occurs on a fault in a single earthquake. A rupture length of 12 km (7.5 miles) was used based on the length of the Coronado fault shown in Kennedy and Welday (1980) and Treiman (1993). The calculated average displacement was 26 cm and the maximum displacement was 36 cm. The sense of slip is not implied in this model, so it was assumed it could be either right lateral or left lateral with a normal component.

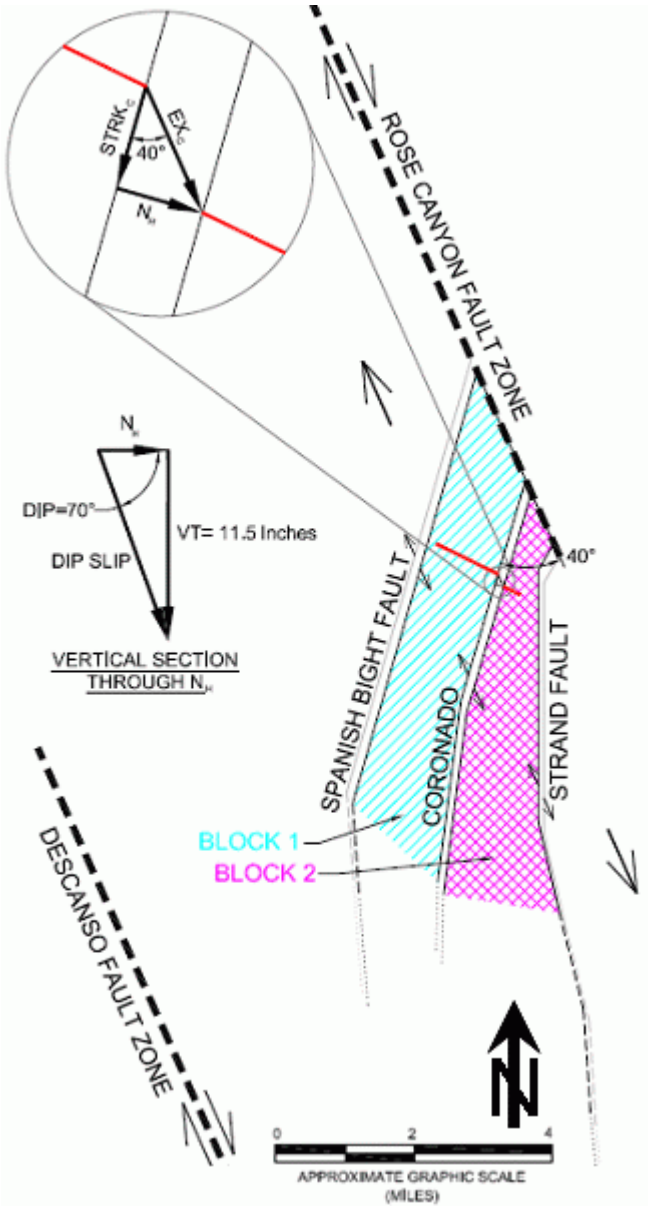

Fig. 9. Diagram showing extensional faulting kinematic model geometry and sense of movement.

Extensional Faulting Kinematic Model

The topographical low of the San Diego Bay has been interpreted to have resulted from extension in a pull apart basin formed by the right step cross over from the northern terminus of the offshore Descanso fault to the southern terminus of the Rose Canyon fault (Abbott, 1999; Kennedy and Clarke, 2001). Normal faulting is typically associated with pull-apart basin formation, as has been observed for the Spanish Bight, Coronado, and Silver Strand faults in this and other studies (Kennedy and Clarke, 1999, 2001; Treiman, 2002, 2003). In a right lateral, right stepping, pure extensional pull apart basin, cross faults will probably be oblique faults with normal and right lateral displacement components (Rodgers, 1980).

A structural model was developed to analyze the kinematics of the extensional pull apart basin. The model is bordered on the east by the Rose Canyon fault and to the west by the parallel striking Descanso fault. The Spanish Bight and Coronado faults branch off of the Rose Canyon fault at an angle of 40 degrees. The Silver Strand fault runs subparallel to the Coronado fault. "Block 1" in the model is formed by the Rose Canyon fault, Spanish Bight fault, and Coronado fault, and "Block 2" is formed by the Coronado fault, and the Spanish Bight fault. Theoretically, Block 1 and Block 2 extend to the Descanso fault to the south-southwest, however, the actual continuity of the blocks toward the Descanso fault is not well defined. The trend of the Coronado fault in the vicinity of the project alignment forms an angle of about 40 degrees with the general trends of the Rose Canyon fault and Descanso faults. The geometry of the structural model was developed based on mapping by Treiman (1993).

The kinematics of this model permit vertical throw to be mathematically related to strike slip offset. Using the dip (DIP) of 70 degrees ascertained from the field investigation and assuming the blocks separate from each other in the direction parallel to the RCFZ, the strike slip displacement ($STRK_C$) can be calculated as follows:

$STRK_C = N_H/\tan(40°)$, where:

N_H = VT/tan(DIP) = horizontal component of dip slip;

VT = 29 cm = vertical throw measured in trench

The geometric basis of these relationships is presented in Figure 9. Using these relationships, a right lateral strike slip offset of about 13 cm was calculated.

It should be noted that the extensional model predicts a horizontal throw (horizontal extension parallel to the general trend of the Rose Canyon fault) on the Coronado fault of about 17 centimeters, which is substantially less than the expected per-event strike slip offset estimated for the Rose Canyon fault by Rockwell and Murbach (1999) of 3 m. However, this small Coronado fault horizontal extension relative to the per-event strike slip for the Rose Canyon fault is not unexpected considering: 1) Pull-apart structures account for a significant percentage of major rupture terminations (Knuepfer, 1989) and step-overs larger than about 5 km in width are rarely or

never ruptured through (Wesnousky, 2008). Thus, in this model, San Diego Bay is a likely termination zone for large Rose Canyon fault surface ruptures and the expected amount of displacement will likely be much less than 3 m; and 2) It is rare to be able to transfer all displacement through areas of structural complexity. In large earthquakes, zones of structural complexity commonly express much less recognizable displacement. For instance, in the 1999 Izmit rupture in Turkey, 5 m of slip in the city of Gulcuk decreased to about 2 m of dip slip and 1.2 m of strike slip at a releasing (extensional) step-over immediately east of Gulcuk (Barka et al., 2002).

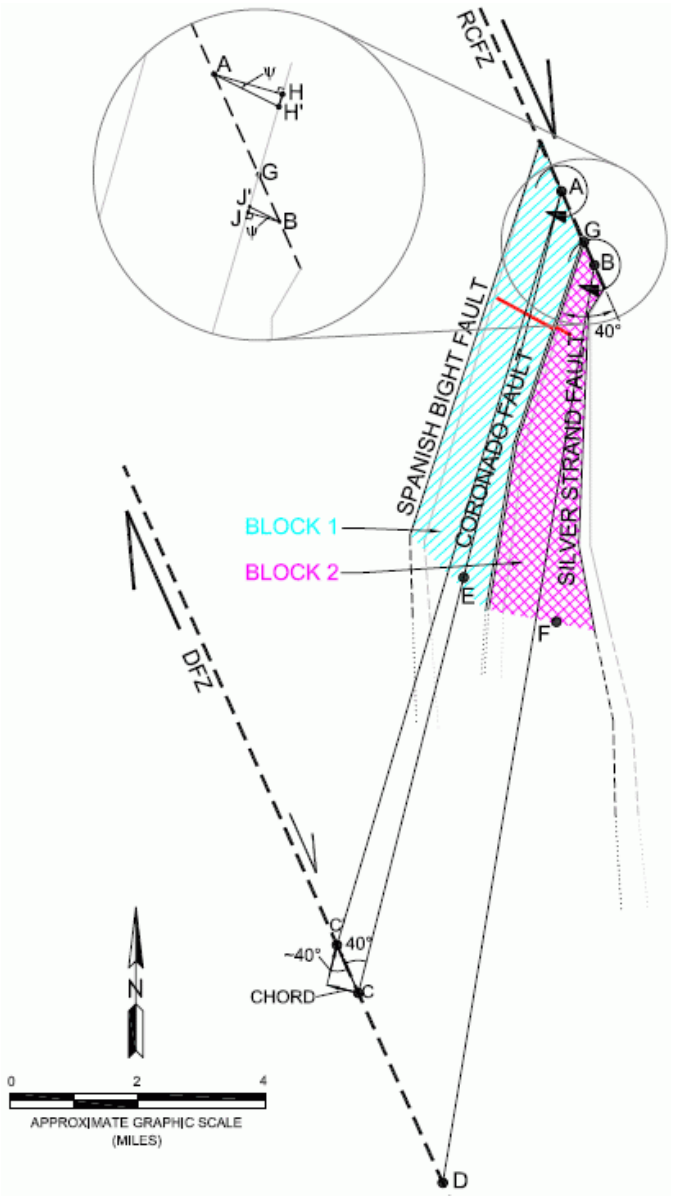

Fig. 10. Diagram showing wrench faulting kinematic model geometry and sense of movement.

Wrench Faulting Kinematic Model

A wrench fault kinematic model was developed with the same geometry as the extensional model. However, rather than accommodating the strain of the right lateral step over between the Descanso fault and Rose Canyon fault by pure extension, this model assumes a wrenching action that rotates Block 1 and Block 2 in a counterclockwise direction. This counterclockwise rotation results in left lateral strike slip on the Spanish Bight, Coronado, and Silver Strand faults. As mentioned earlier, previous small earthquakes within the San Diego Bay that occurred from 1985 to 1987 have suggested that left lateral strike slip is possible along northeast-striking faults in the area of the San Diego Bay (Magistrale, 1993).

In Case 1 of this model, Block 1 and Block 2 were assumed to be pinned where they meet the Rose Canyon fault and Descanso fault. Blocks 1 and 2 are pinned at the Rose Canyon fault and at the midpoint between the Rose Canyon fault and Descanso fault in Case 2. These two pinning scenarios are intended to account for uncertainty in the continuity of the blocks to the Descanso fault. Three meters of wrenching movement between the Rose Canyon fault and Descanso fault was imposed on the model. The block rotation and left lateral strike slip along the Coronado fault were then calculated based on the wrenching movement as follow. The geometric basis for the calculations is presented in Figure 10.

CHORD = CC'·sin(40°) = (3 m)· sin(40°) = 1.93 m

AC = 20,760 m

AE = AC/2 = 10,380 m

Case 1 – Rotation About Points A, B, C and D:

ψ_1=arctan(CHORD/AC) = arctan(1.93m/20,760m) = 0.00533°

STRK = HH' + JJ' = AH·tan(ψ_1) + BJ·tan(ψ_1)

STRK = (896 m + 418 m)·tan(0.00533°) = 12 cm

Case 2 – Rotation About Points A, B, C and D:

ψ_1=arctan(CHORD/AE) = arctan(1.93m/10,380m) = 0.0107°

STRK = HH' + JJ' = AH·tan(ψ_2) + BJ·tan(ψ_2)

STRK = (896 m + 418 m)·tan(0.0107°) = 25 cm

Case 1 resulted in 12 cm of left lateral strike separation on the Coronado fault and Case 2 resulted in 25 cm of left lateral strike separation on the Coronado fault.

"Horsetail" Model

A "horsetail" model was developed that assumes right lateral strike slip fault displacement on the main trace of the Rose

Canyon fault is transferred to the Spanish Bight, Coronado, Silver Strand, and un-named faults mapped in the bay around the San Diego-Coronado bridge. The geometric basis for this model is presented in Figure 11. Data is not available that would suggest uneven partitioning between these four recipients of slip from the Rose Canyon fault, so the model assumed that each receives an equal amount. Rockwell and Murbach (1999) estimate 3 m of right lateral slip per event on the main trace of the Rose Canyon Fault. Therefore the model assigns 75 cm (3 m divided by 4) of Rose Canyon fault-parallel horizontal throw to the Coronado fault. This horizontal throw is then converted to strike slip on the Coronado fault using the angle of incidence between the main trace of the Rose Canyon and Coronado faults of 40 degrees.

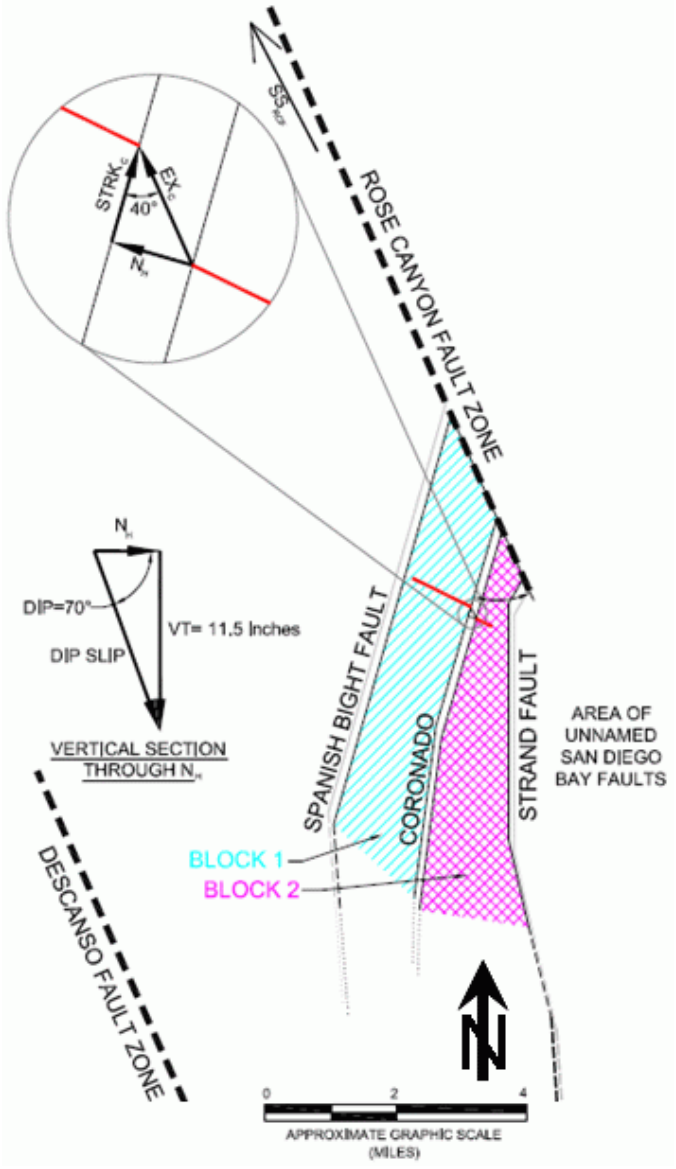

Fig. 11. Diagram showing "horsetail" faulting kinematic model geometry and sense of movement.

$STRK_C = (3\ m)/4 \cdot \cos(40°) = 57$ cm

This results in 57 cm of right lateral strike slip displacement per event on the Coronado fault.

SUMMARY OF FAULT OFFSET USED FOR DESIGN

For design we conservatively assumed that the 29 cm of vertical throw that was determined from the fault trenching could occur in a single event. While the fault trench data suggested that faulting was concentrated in a 1.2 m wide zone, we conservatively assumed the "main zone" of faulting occurred over a 0.6-meter width.

The strike slip estimates made using the four techniques described above are summarized in Table 1. These estimates range from 25 to 36 cm of left lateral displacement, to 25 to 57 cm of right lateral displacement. The design offsets for the main fault zone were taken as the maxima of the range: 36 cm of left lateral displacement and 57 cm of right lateral displacement. The left lateral and right lateral modes were considered as two possible scenarios.

Table 1. Summary of strike slip displacement estimates

Model/ Method	Minimum Displmt.	Mean Displmt.	Maximum Displmt.	Displacement Displmt.
Wells & Coppersmith (1994)	---	26 cm	36 cm	Right or Left Lateral
Extensional Fault	*Best Estimate:* 13 cm			Right Lateral
Wrench Fault	12 cm	---	25 cm	Left Lateral
"Horsetail"	*Best Estimate:* 57 cm			Right Lateral

Similar to the normal offset case, it was considered prudent to consider some secondary strike slip offset outside of the main zone in the tunnel design. Based on a review of literature describing post-earthquake field reconnaissance, laboratory models, numerical models and empirical techniques for estimating secondary offset (Bray, 2001; Bray, 2005; Bray and Kelson, 2006; Kelson et al., 2004; Petersen et al., 2005), estimates of secondary displacement off of the main trace were developed for design.

Peterson et al. (2005) present an empirically derived equation for estimating secondary displacements on one side of a strike slip fault as a percentage of the main zone displacement. Their mean plus two standard deviations estimate (98 percentile value) of secondary displacement as a percentage of main zone displacement is 57 percent. Fifty percent secondary fault displacement on both side of the active zone was conservatively adopted for use in design for this project.

Using the 50 percent secondary displacement rule, the secondary displacement was 28 cm for the right lateral

scenario and 18 cm for the left lateral scenario. The secondary offsets were linearly distributed over a 15.2-m width on the hanging wall side of the main zone and a 15.2-m width on the footwall side of the main zone.

Figure 12 a, b and c show the distribution of right lateral strike slip, left lateral strike slip and vertical throw, respectively, that was used for design. The offset distribution is with respect to an imaginary horizontal line drawn perpendicular to the fault strike.

APPLICATION OF FAULT OFFSET TO TUNNEL DESIGN

The design free field fault offsets were used as input to soil structure interaction (SSI) analyses of the tunnel alternatives. Two types of analyses were performed: Winkler-type beam on non-linear foundation analyses and continuum finite difference analyses. For the Winkler analyses it was necessary to translate the free field displacements through vector rotation to axial, transverse lateral and vertical displacements relative to the tunnel axis. Detailed description of the SSI analyses is beyond the scope of this paper. Interested readers are referred to Gregor et al. (2007).

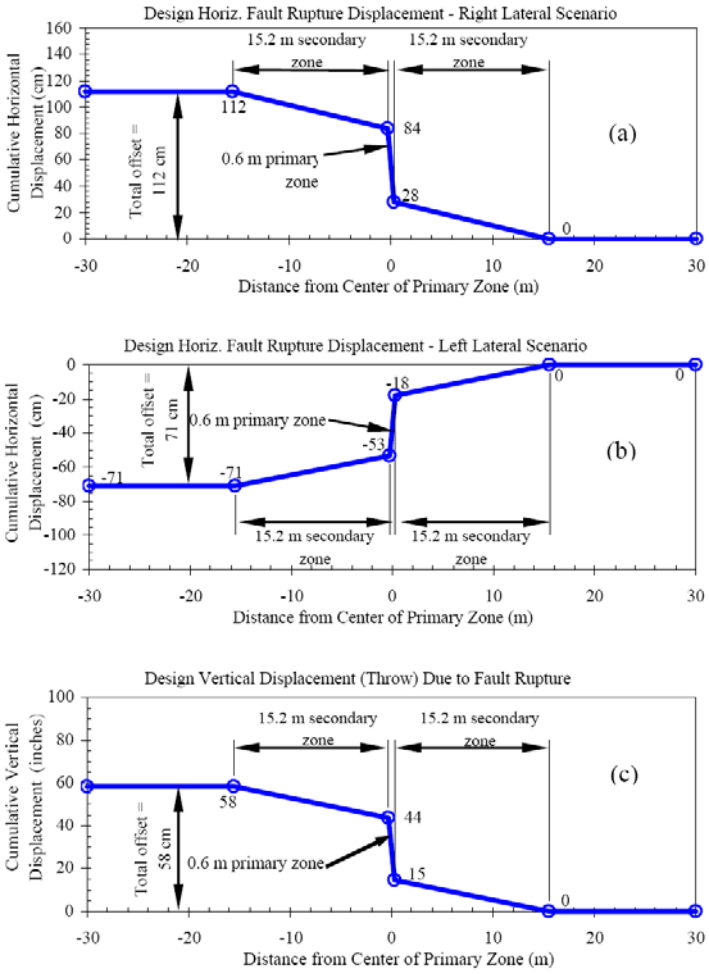

Fig. 12. Distribution of fault displacement used for design.

DISCUSSIONS AND CONCLUSIONS

A phased approach to field investigation was adopted for this study. Four principal investigation methods were employed in the following order: a seismic reflection survey, large diameter borings, closely-spaced cone penetrometer tests (CPT) and a fault trench.

Closely spaced CPTs and a fault trench were successful in definitively locating the Coronado fault. This study is the first to confirm the location and active status of the Coronado fault on land. It was also shown that the scarp which traverses Coronado is associated with normal displacement of the Coronado fault.

Logging of pedogenic soil horizons in the fault trench showed evidence that approximately 29 cm of Holocene vertical throw has occurred on the Coronado fault. The fault trench logging also showed evidence that strike slip displacement has occurred on the Coronado fault.

Strike slip displacements were estimated for project design purposes using four models: an independent rupture model; and extensional pull-apart model; a wrench fault model; and a "horsetail" model. The models provided strike slip estimates ranging from 25 to 36 cm of left lateral displacement, to 25 to 57 cm of right lateral displacement.

Several fault rupture scenarios were developed for design of the proposed tunnel structures. These design scenarios included zones of secondary faulting in addition to the primary faulting. The fault rupture scenarios were incorporated into preliminary engineering and design for the proposed tunnel options.

ACKNOWLEDGEMENTS

The authors would like to acknowledge our project partners. Kleinfelder served as a subconsultant to the prime consultant, Parsons Brinckerhoff (PB). Earth Consultants International was a subconsultant to Kleinfelder. Hatch Mott MacDonald served as the tunnel engineering sub-consultant to PB. The owner was the City of Coronado and Caltrans served as the lead reviewer.

REFERENCES

Abbott, P.L. [1999]. *The Rise and Fall of San Diego*, Sunbelt Publications, Inc., 231 p.

Artim, E.R. and Streiff, D. [1981]. *Trenching the Rose Canyon Fault Zone, San Diego, California*, U.S. Geological Survey Contract No. 14-08-0001-19118.

Barka, A., Akyuz, H.S., Altunel, E., Sunal, G., Cakir, Z., Dikbas, A., Yerli, B., Armijo, R., Meyer, B., Chabalier, J.B., Rockwell, T., Dolan, J.R., Hartlieb, R., Dawson, T., Christofferson, S., Tucker, A., Fumal, T., Langridge, R., Stenner, H., Lettis, W., Bachhuber, J., and Page, W. [2002]. "The surface rupture and slip distribution of the 17 August 1999 Izmit earthquake (M7.4), North Anatolian fault", *Bulletin of the Seismological Society of America, Special Issue on the 1999 Izmit and Duzce, Turkey, Earthquakes*, N. Toksoz (ed.)., v. 92, no. 1, p. 43-60.

Bennett, R, A. et al. [1996]. "Global positioning system constraints on fault slip rate in Southern California and Northern Baja, Mexico," *Journal of Geophysical Research*, vol. 101, no. B10, pp. 21,943-21,960.

Bray, J. D. [2001]. "Developing mitigation measures for the hazards associated with earthquake surface fault rupture", *Seismic Fault-Induced Failures Workshop*, Japan Society for the Promotion of Science, University of Tokyo, Japan, pp. 55-79, January 11-12, 2001.

Bray, J.D., [2005]. unpublished Caltrans Technical Advisory Panel review comments

Bray, J.D. and K.I. Kelson, [2006]. "Observations of Surface Fault Rupture from the 1906 Earthquake in the Context of Current Practice," *Earthquake Spectra, Earthquake Engineering Research Institute*, April 2006, Vol. 22, No. S2, pp. S69-S89.

California Geological Survey (CGS) [2003]. *Earthquake Fault Zone Map, Point Loma Quadrangle*, Scale 1:24,000.

Caltrans [1998]. "San Diego Coronado Bay Toll Bridge, seismic retrofit project 618, design contract no. 59X487, expedite structure plans, prepared by McDaniel Engineering/J. Muller International for California Department of Transportation", sheets 1-16 and 197-277 showing boring locations and boring logs, various scales, February 11, 1998.

Gregor, T., Garrod, B., Young, D.J. [2007]. "Analyses Of Underground Structures Crossing An Active Fault In Coronado, California", *International Tunneling Association Conference*, June 25-28, 2007, Prague, Czech Republic.

Hatch Mott MacDonald (HMM) [2007]. *Advance Planning Study (APS), SR 75/282 Transportation Corridor – Fourth Street Tunnel Alternatives*. Consultant report, April 2007.

Heusser, L. [1978]. "Pollen in Santa Barbara Basin, California: A 12,000-yr record", *Geological Society of America Bulletin*, v. 89, p. 673-678.

Kelson, K.I., Hitchcock, C.S., Baldwin, J.N., Hart, J.D., Gamble, J.C., Lee, C-H and Dauby, F., [2004]. "Fault Rupture Assessments for High-Pressure Pipelines in the Southern San Francisco Bay Area, California", *Proceedings of the International Pipeline Conference*, October 4-8, 2004, Calgary, Alberta, Canada.

Kennedy, G.L. [2006]. "Paleontological assessment of late Pleistocene marine fossils from Glorietta Bay and vicinity, Coronado, San Diego County, California", consultant report prepared for Kleinfelder.

Kennedy, M.P. and Clarke, S.H. [2001]. "Late Quaternary Faulting in San Diego Bay and Hazard to the Coronado Bridge", *California Geology*, July/August.

Kennedy, M.P. and Welday E.E. [1980]. *Character and Recency of Faulting Offshore Metropolitan, San Diego, California*, CDMG map sheet 40.

Kern, J.P. and Rockwell, T.K. [1992]. "Chronology and deformation of Quaternary marine shorelines, San Diego County, California", *Quaternary Coasts of the United States: Marine and Lacustrine Systems*, Society of Economic Paleotologists and Mineralogists Special Publication No. 48, p. 377-382.

Kleinfelder [2006]. *Final Preliminary Engineering Geotechnical Investigation, Vol. I & II. State Route 75 and 282 Transportation Corridor Project, Coronado, California*. Consultant's report, April 12, 2006.

Knuepfer, P.K., [1989]. "Implications of the characteristics of end-points of historical surface ruptures for the nature of fault segmentation", *U.S. Geological Survey Redbook on Fault Segmentation and the Controls of Rupture Initiation and Termination*, U.S. Geological Survey Open File Report 89-315, p. 193-221.

Lindvall, S.C. and Rockwell, T.K. [1995]. "Holocene activity of the Rose Canyon Fault Zone in San Diego, California", *Journal of Geophysical Research*, vol. 100, no. B12, pp. 24,121 – 24,132.

Magistrale, H., [1993]. "Seismicity of the Rose Canyon Fault Zone near San Diego, California", *Bulletin of the Seismological Society of America*, Vol. 83, No. 6, pp. 1971-1978.

Peterson, M., Cao, T., Dawson, T., Frankel, A., Wills, C. and Schwartz, D., [2005]. "Mapping Fault Ground Rupture Hazard for Strike Slip Faults" – May 16, 2005 Draft, to be published as a Pacific Earthquake Engineering Research Center (PEER) report.

Rockwell, T.K., Johnson, D.L., Keller, E.A. and Dembroff, G.R. [l985]. "A late Pleistocene-Holocene soil chronosequence in the central Ventura Basin, Southern California, U.S.A.", in K. Richards, R. Arnett, and S. Ellis (eds.), *Geomorphology and Soils*, George Allen and Unwin, p. 309-327.

Rockwell, T.K. [2000]. "Use of soil geomorphology in fault studies: in Quaternary Geochronology: Methods and Applications", J.S. Noller, J.M. Sowers, and W.R. Lettis, eds, *AGU Reference Shelf 4*, American Geophysical Union, Washington D.C., p. 273-292.

Rockwell, T.R. and Murbach, M., [1999]. *Holocene Earthquake History of the Rose Canyon Fault Zone, Final Technical Report Submitted for USGS*, Grant No. 1434-95-G-2613, 37 pp.

Rodgers, D.A., [1980]. *Analysis of pull-apart basin development produced by en echelon strike-slip faults*, in P.F. Balance and H.G. Reading, eds., Oxford, England, International Association of Sedimentologists, p. 27-41.

Treiman, J. A., [1993]. "The Rose Canyon Fault Zone Southern California", *California Division of Mines and Geology Open-File Report 93-02*, Plate 1.

Treiman, J.A. [2002, 2003]. *Fault Evaluation Report FER-245, Silver Strand Fault, Coronado Fault, Spanish Bight Fault, San Diego Fault, and Downtown Graben, Southern Rose Canyon Fault Zone, San Diego, California with supplement No. 1*, California Department of Mines and Geology unpublished report.

Wells, D.L., and Coppersmith, K.J., [1994]. "New empirical relationships among magnitude, rupture length, rupture width, rupture area, and surface displacement", *Bulletin of the Seismological Society of America*, Vol. 84, No. 4, pp. 974-1002, August, 1994.

Wesnousky, S. [2008]. "Displacement and geometrical characteristics of earthquake surface ruptures: Issues and implications for seismic-hazard analysis and the process of earthquake rupture", *Bulletin of the Seismological Society of America*, Vol. 98, No. 4, pp. 1609-1632.